Engineering Applications of Computational Fluid Mechanics Vol. 7, No.1, pp. 131–143 (2013)

IDENTIFICATION AND SUPPRESSION OF NOISE SOURCES AROUND HIGH SPEED TRAINS

Zhenxu Sun *†, Dilong Guo *, Shuanbao Yao *, Guowei Yang * and Minggao Li #

* *Key Laboratory for Mechanics in Fluid Solid Coupling Systems, Institute of Mechanics, C A S, No.15 Beisihuanxi Road, Beijing 100190, China*
† *E-Mail: sunzhenxu@imech.ac.cn (Corresponding Author)*
# *Tangshan Railway Vehicle Co., Ltd., Tangshan 063000, China*

ABSTRACT: Aerodynamic noise would become a significant limiting factor as the running speed of high speed trains increases, and should be taken into consideration during the design of high speed trains. In the present work, the Nonlinear Acoustics Solver (NLAS) has been adopted to investigate the aerodynamic noise of high speed trains. The region around the streamlined head of the leading car and the trailing car, the bogie region, the upstream zone and the wake zone are discussed and the distribution characteristics of aerodynamic noise sources around a high speed train is exhibited. The acoustic characteristics of the streamlined head could be contaminated due to the unreasonable arrangement of cab windows or cowcatchers. As a result, different designs of cab windows and cowcatchers are investigated in this paper and advice on low noise design is given. Based on the above analysis, a new design of the streamlined head is proposed. Numerical results reveal that the noise level of the new streamline has been greatly suppressed. The analysis would aid in identification of noise sources around high speed trains and design of high speed trains with low noise.

Keywords: aerodynamic noise, NLAS, high speed trains, low noise design

1. INTRODUCTION

Generally speaking, the study on the noise of high speed trains is mainly on the study of noise sources, including the location and clarification of noise sources (Talotte et al., 2003). Generally two kinds of sources have been identified, namely rolling noise and aerodynamic noise. The former mainly refers to mechanical noise, which is induced by wheel vibration and rail vibration (Moritoh et al., 1996). The latter mainly considers the noise induced by the surfaces in the flow field. Two kinds of noise sources have been identified (Talotte, 2000): one is that radiated by the steady flow structures. For example, the steady vortex shedding just behind the pantograph can generate significant aerodynamic noise, which contributes a major part of the noise. Besides, some cavity structures on the surface of high speed trains can also generate aerodynamic noise. For example, the inter-coach spacing and the recess of the pantograph on TGV high speed trains in France are both cavity noise sources (Noger et al., 2000). The other one is that emitted by turbulent fluctuations, which mostly locates in the turbulent boundary layer around the surface of high speed trains or in places where flow separations take place. Once the locations of the noise sources have been determined, ways to suppress the noise sources and reduce the noise level should then be considered. The sound power of aerodynamic noise increases with the sixth order of the running speed. As the speed of high speed trains increases, the contribution of aerodynamic noise becomes predominant (Mellet et al., 2006). As a result, when the train is running at a high speed, the overall noise level can never be reduced if only the reduction of mechanical noise is considered. In this situation the aerodynamic noise must be taken into consideration.

Experiments and numerical simulations are two commonly used approaches to the study of aerodynamic noise of high speed trains. The former can be classified into two kinds, namely the real vehicle tests and wind tunnel investigations on scaled models (Moritoh et al., 1996; Nagakura, 2006). However, real vehicle tests and wind tunnel investigations suffer a lot for specific reasons, for example, manpower and material resources. With the development of modern computers, numerical simulations are gradually accepted to predict the aerodynamic noise. To numerically simulate the aerodynamic noise, currently two commonly used methods exist in computational aero-acoustics. The direct simulation is a common choice, which includes direct numerical simulation (DNS), large eddy simulation (LES), and unsteady RANS (URANS)

Received: 27 Mar. 2012; Revised: 14 Sep. 2012; Accepted: 3 Nov. 2012

simulation. DNS and LES suffer from their large requirement on grids, which limits their practical application. On the contrary, URANS could satisfy the need for grids in engineering problems, but it could bring relatively large numerical error due to its failure in capturing the sources in sub-grid scales. The second approach is the acoustic analogy methods. It was originated from Lighthill, which is known as the Lighthill equation (Lighthill, 1952 and 1954). Later on, Curle (1955) solved the Lighthill equation within a solid boundary. Then Ffowcs-Williams and Hawkings (1969) extended Curle's solution to the moving boundary, and derived the famous FW-H equation. Casper and Farassat (2002) have done a thorough research on FW-H equation and useful formulas have been obtained. This approach has an obvious advantage in predicting far field noise due to its independence on mesh resolution for far field probes and even far field probes do not need to be included in the computational domain.

A reasonable choice of computational algorithm is crucial to the prediction of aerodynamic noise of high speed trains. The nonlinear acoustics solver method (NLAS), which is derived from Batten et al. (2002 and 2004), has been chosen to predict aerodynamic noise in the near field. It is a nonlinear method and its requirement for grids can be relaxed on the near wall. Reconstruction of turbulence variables takes the sub-grid sources into consideration, which could both reduce the grid need and maintain the computational accuracy (Batten et al., 2002 and 2004).

In the present paper, the characteristics of noise sources of high speed trains have been numerically studied, and the near field feature of noise sources is emphasized. Two specific noise sources around the streamline, cab windows and cowcatchers, are mainly discussed. In order to suppress the noise level around these regions, some designs are proposed and best the low noise design of high speed trains is suggested. Furthermore, noise analysis of the best design has been performed.

2. ALGORITHMS

2.1 RANS model

The transient calculation should be performed on the premise of the steady RANS calculation of the flow field. Through the RANS calculation, the statistical steady mean flow could be obtained, from which the main generation zone of turbulence could be revealed. In the present paper, an anisotropic turbulence model, the cubic $k-\varepsilon$ model, is utilized so as to preferably model the statistically steady flow field (Merci et al., 2001). Non-linear terms are taken into consideration to account for normal-stress anisotropy, swirl and streamline curvature effects. Consequently, the local Reynolds-stress tensor could be provided precisely so as to synthesize the noise sources.

2.2 Nonlinear acoustics solver

NLAS is designed to model noise generation and propagation from an initial statistically-steady model of turbulent flow data. A reconstruction procedure is performed to generate noise sources from the given set of statistics. Moreover, NLAS is a low diffusive solver and can model the generation of noise in sub-grid scales. NLAS assumes the perturbation to be added into NS equations, in which quantities are split into mean and fluctuating parts. The perturbation equations then could be obtained as follows, which is usually referred to as non-linear disturbance equations (NLDE):

$$\frac{\partial Q'}{\partial t}+\frac{\partial F_i'}{\partial x_i}-\frac{\partial (F_i^{\upsilon})'}{\partial x_i}=-\frac{\partial \overline{Q}}{\partial t}-\frac{\partial \overline{F}_i}{\partial x_i}+\frac{\partial \overline{F}_i^{\upsilon}}{\partial x_i}$$

$$\overline{Q}=\begin{bmatrix}\overline{\rho}\\ \overline{\rho}\overline{u}_j\\ \overline{e}\end{bmatrix},\overline{F}_i=\begin{bmatrix}\overline{\rho}\overline{u}_i\\ \overline{\rho}\overline{u}_i\overline{u}_j+\overline{p}\delta_{ij}\\ \overline{u}_i(\overline{e}+\overline{p})\end{bmatrix},\overline{F}_i^{\upsilon}=\begin{bmatrix}0\\ \overline{\tau}_{ij}\\ -\overline{\theta}_i+\overline{u}_k\overline{\tau}_{ki}\end{bmatrix}$$

$$Q'=\begin{bmatrix}\rho'\\ \overline{\rho}u_j'+\rho'\overline{u}_j+\rho'u_j'\\ e'\end{bmatrix},\left(F_i^{\upsilon}\right)'=\begin{bmatrix}0\\ \tau_{ij}'\\ -\theta_i'+u_k'\overline{\tau}_{ki}+\overline{u}_k\tau_{ki}'\end{bmatrix}$$

$$F_i'=\begin{bmatrix}\overline{\rho}u_i'+\rho'\overline{u}_i\\ \rho'\overline{u}_i\overline{u}_j+\overline{\rho}\overline{u}_iu_j'+\overline{\rho}u_i'\overline{u}_j+p'\delta_{ij}\\ u_i'(\overline{e}+\overline{p})+\overline{u}_i(e'+p')\end{bmatrix}+\begin{bmatrix}\rho'u_i'\\ \overline{\rho}u_i'u_j'+\rho'u_i'\overline{u}_j+\rho'\overline{u}_iu_j'+\rho'u_i'u_j'\\ u_i'(e'+p')\end{bmatrix}$$

Neglecting density fluctuations and taking time averages gives:

$$\overline{LHS}=\overline{RHS}=\frac{\partial R_i}{\partial x_i}$$

Fig 1 Prototype model of CRH3 high speed train.

$$R_i = \begin{bmatrix} 0 \\ \bar{\rho}\overline{u_i' u_j'} \\ c_p \overline{\rho T' u_i'} + \bar{\rho}\overline{u_i' u_k'}\bar{u}_k + \frac{1}{2}\bar{\rho}\overline{u_k' u_k' u_i'} + \overline{u_k' \tau_{ki}} \end{bmatrix}$$

The above terms correspond to the standard Reynolds-stress tensor and turbulent heat fluxes.

3. COMPUTATIONAL MODEL, MESH AND CONDITIONS

The prototype of CRH3 high speed train is considered in the present paper, with a leading car, a middle car and a trailing car. The characteristics of noise sources are investigated and the streamlined head, cab windows and bogies are mainly discussed. The CRH3 model is shown in Fig. 1.

It is worth mentioned that the inter-spacing between adjacent carriages is also an important noise source. However, the study of this kind of noise sources has been investigated in details in literature (Sun et al., 2012). As a result, it will not be discussed in the present paper. Specific structures around the streamline are shown in Fig. 2.

In the following analysis of low noise designs, some other types of cab windows and cowcatchers are considered, and numerical simulations of these cases are carefully performed. Based on the above analysis, a best low noise design of high speed trains has been derived and further acoustic analysis on this new design has been performed.

Taking L as the length of the high speed train, the upstream length is set as 1L while the downstream length of the domain is set as 2L. The width and height of the domain are set as 0.8L and 0.53L respectively, just as Fig. 3 shows.

The commercial software package ICEM is utilized for mesh generation. Due to the complicated geometry used in the present paper, the hybrid mesh is adopted. Considering the balance between the computational efficiency and accuracy, the amount of the total grids is controlled at around 12 million. Specific positions are densified so as to better model the characteristics of the geometry and capture the local flow characteristics. For example, considering intensive turbulence exists in the wake zone, finer mesh should be used compared to adjacent zones. The mesh configuration of current model is the same as the previous model in Sun et al. (2012), with its y-plus around walls locating in a range of 30-100. As a result, the accuracy of the steady calculation of the flow field and the transient calculation of the aerodynamic noise could both be ensured, since the NLAS approach has the least requirement for mesh resolution (Batten et al., 2004). The surface mesh on the streamlined head and the leading bogie are shown in Fig. 4.

When statistically steady RANS calculation is performed, the uniform flow condition is utilized with a speed of 250 km/h at the inlet boundary, and the ground is set to be a moving wall with the

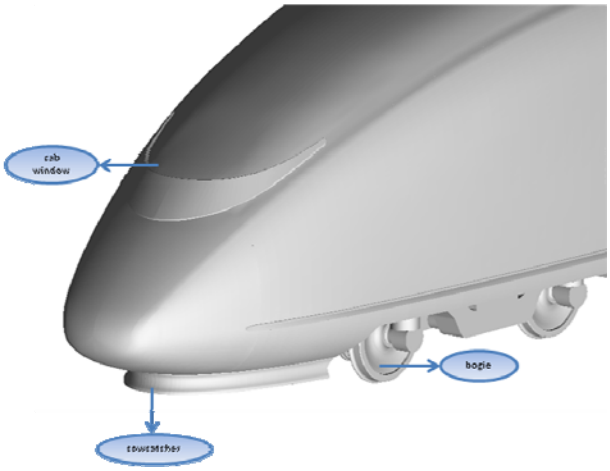

Fig. 2 Specific structures around streamline.

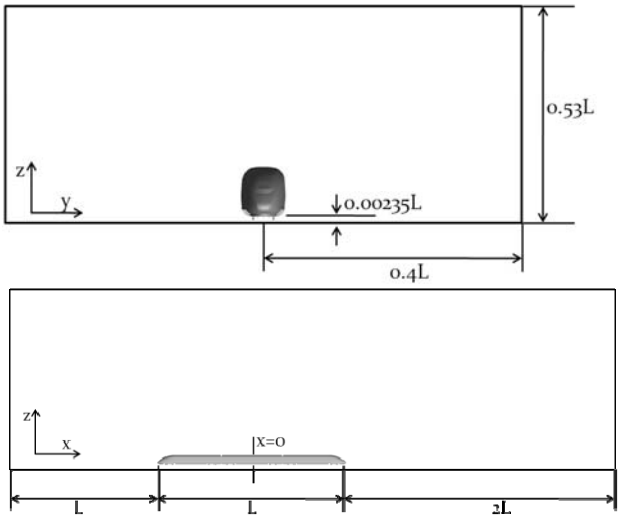

Fig. 3 Computational domain.

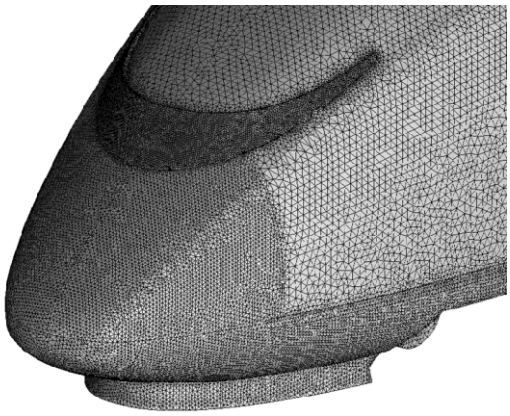

(a) surface mesh on streamlined head

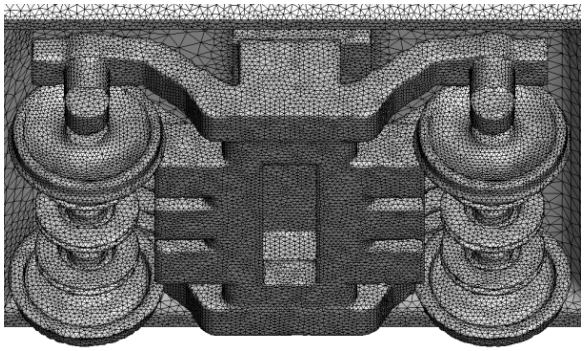

(b) surface mesh on leading bogie

Fig. 4 Surface mesh at specific locations.

same speed as the inlet boundary. The pressure outlet condition is imposed at the outlet boundary with a 0 Pa gauge pressure. The reference pressure is set to be 1 atm. When the NLAS procedure is conducted, 3 absorbing layers are imposed on the inlet boundary, the outlet boundary and the far field boundary to prevent wave reflections from these boundaries. 200 Fourier modes are set to perform synthetic reconstruction for the turbulent fluctuating quantities so as to capture the sub-grid sources correctly. The time step in NLAS simulation is set to 2e-5s, and the simulated physical time is 0.3s, which insures that the noise whose frequencies locate between 10-10000Hz could be precisely predicted.

4. RESULTS AND DISCUSSIONS

The characteristics of noise sources of high speed trains in the near field are firstly discussed based on a specific case. The streamlined head (both the leading car and trailing car), the bogies, the upstream and the wake zone are the main concern. As a result, the distribution characteristics of noise sources of the high speed train could be obtained. For those specific noise sources, cab windows and cowcatchers, comparative study among different designs is then conducted.

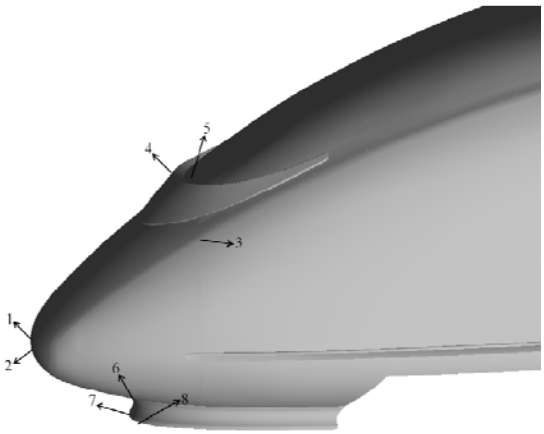

Fig.5 Probe configuration on streamlined head.

4.1 Acoustic characteristics in near field

Based on the statistical results obtained by RANS simulation, synthetic reconstruction of turbulent quantities can be accomplished by NLAS approach, which could be used to predict aerodynamic noise. Near field noise could be directly obtained through these fluctuating variables with the FFT tool. In the following sections, analysis of noise sources of different locations will be performed.

4.1.1 Streamlined head of leading car

In spite of the running speed, the aerodynamic noise of high speed trains are mainly determined by the streamlined head and some attached components as well. Better streamlined head and smooth connection between different parts could suppress the aerodynamic noise apparently. In this section the streamlined head of the leading car are the main concern and several probes are imposed on top of the surface of the streamlined head, as Fig 5 shows.

Probes 1 and 2 are just on top of the nose of the streamlined head, so as to study the noise characteristics of the streamline. Probe 3 locates on the side of the streamlined head, where the flow experiences a higher speed and generates higher turbulence intensity. The connection between the cab window and the streamline has a crucial influence on the noise level of the streamline. Probes 4 and 5 could be used to investigate the aerodynamic noise feature around the cab window. Probes 6, 7 and 8 locate around the cowcatcher, just below the nose of the streamline, which will be used to study the noise caused by the cowcatcher. Frequency spectrums of A-weighted sound pressure of these probes are shown in Fig. 6.

As Fig. 6a shows, probe-1 locates just on top of the nose, where exists a distinct frequency peak of

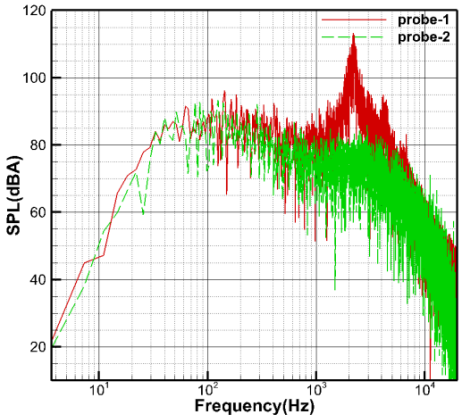

(a) frequency spectra around nose

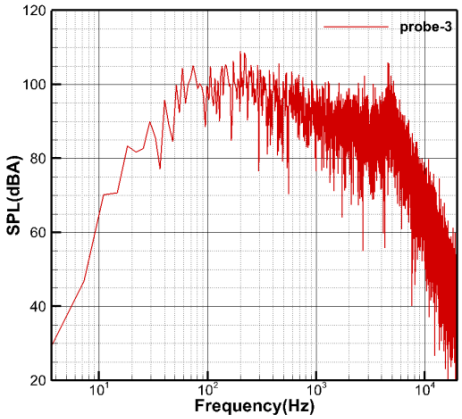

(b) frequency spectra at side of streamline

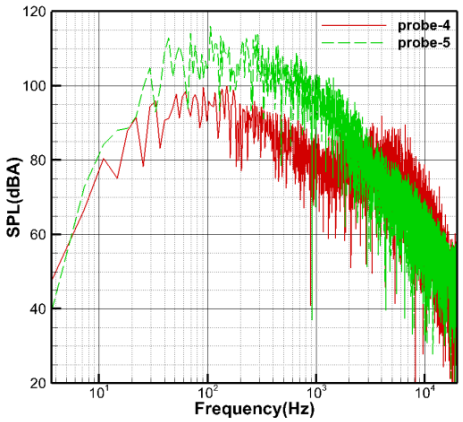

(c) frequency spectra around cab window

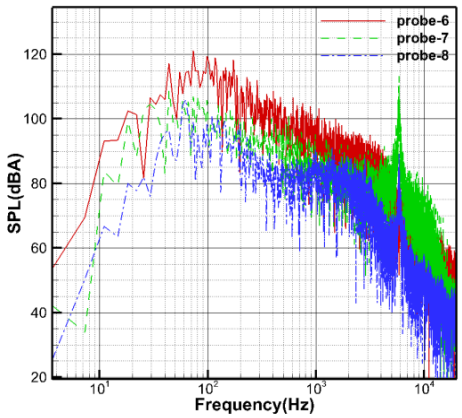

(d) frequency spectra around cowcatcher

Fig. 6 Frequency spectra around streamline of leading car.

2100Hz and a corresponding sound pressure level of 113 dB. However, the aerodynamic noise in the zone just below the nose, indicated by probe-2, has no obvious dominant frequency. As a kind of broadband noise, the energy-contained frequencies mainly gather in the middle and high frequency band, ranging from 80-3000Hz, with a SPL of around 80 dBA. Compared to probe-2, probe-1 has a higher sound pressure level in the frequency of 1000-3000Hz, which is mainly a result of the dominant frequency.

As Fig. 6b shows, the frequency spectrum of probe-3 is also a kind of broadband noise, and a frequency peak of 4300Hz could be observed. Probe-3 locates on the shoulder of the streamline, where high curvature exists, leading to the large gradient of flow variables. As a result, the flow here experiences high turbulence. As a kind of aerodynamic noise sources, high turbulence intensity of the boundary layer usually results in high noise level, just as Fig 7 shows. Compared to the probes at the nose of the streamline, higher noise level with a value of around 100 dBA could be observed.

Fig. 6c gives the frequency spectra of probes around the cab window. Probe-4 locates in front of the cab window, and the flow here shows no obvious disturbance by the cab window. However, probe-5 locates just at the bottom of the cavity, where the flow experiences severe turbulence. Through a comparative study, it can be observed that the noise level of probe-4 is slightly lower, ranging from 80dBA to 100dBA. For probe-5 a higher noise level could be observed with a value varying from 100dBA to 120dBA. As a result, higher noise contamination would be triggered by the region where probe-5 locates. It is worth mentioning that higher noise level could still be found at higher frequencies for probe-4, which is in consistence with the probes at the nose of the streamline. However, this phenomenon does not exist for probe-5.

The acoustic characteristics around the cowcatcher could be discovered by placing probes in specific locations. Probe-6 locates at the connection part between the nose and cowcatcher, where a cavity exists. Probe-7 locates just in front of the cowcatcher while probe-8 locates at the bottom of cowcatcher, as Fig. 5 shows. As seen in Fig. 6d, high noise level around 100dBA could be observed at the tip of the cowcatcher. Higher dominant frequency around 6000Hz could be

detected for probe-7, with a corresponding sound pressure level of 113dBA. For probe-8, the same dominant frequency as with probe-7 could be found while its sound pressure level, with a value of 88dBA, is greatly lower than that of probe-7. As the frequency spectrum of probe-6 shows, probe-6 gets a dominant frequency of 100Hz and a corresponding sound pressure level of 120dBA, which is even higher than that of the region where the cab window stands. As described above, flow field characteristics are the root of aerodynamic noise. In order to better understand the nature of high noise level around the cowcatcher, the streamlines passing by the cowcatcher are sketched in Fig 8.

As shown in Fig. 7, the upstream flow is blocked just in front of the cowcatcher and a stagnation zone forms at the connection part between the nose and the cowcatcher, where probe-6 locates. Two strong vortices exist around the cowcatcher. One is stretching along the surface and the other one locating beneath the bottom of the cowcatcher. The vortex cores are both perpendicular to the flow direction. Positive pressure dominates for the upper vortex and negative pressure dominates for the lower vortex. Due to the existence of the vortices, turbulent fluctuations of the flow are aggravated and the local noise has been deteriorated.

In order to study aerodynamic characteristics of noise in the upstream region, two additional probes are placed in front of the nose, with a distance of 1m and 10m. The frequency spectra of these two probes are shown in Fig. 9.

As seen in Fig. 9, the probe which is farther away from the train has the lower noise level, with a value of 80dBA and a corresponding dominant frequency of 300Hz. Meanwhile, some other frequency modes could also be observed, 600Hz, for instance. As the probe goes near the train, the sound pressure level gets bigger. The probe which is 1m away from the train experiences an aerodynamic noise with a level of 85dBA and a corresponding frequency of 100Hz.

4.1.2 Bogie zone

The model used in present paper contains only three carriages. As a result, only six bogies exist in the model. In the present paper, these bogies are named No. 1 to No. 6 sequentially from the leading car to the trailing car.

Among these bogies, the flow passing by bogie No. 1 is the most turbulent, and the surface of the bogie and its cover are all suffered from high pressure. However, when the flow goes

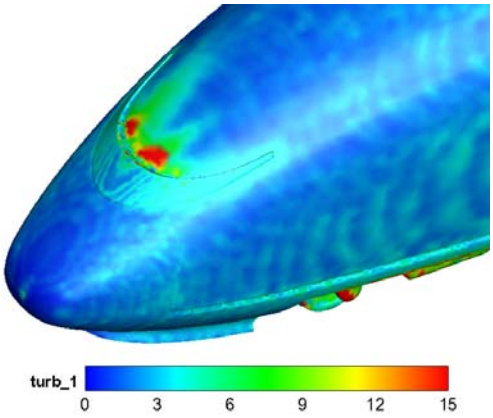

Fig. 7 Turbulence kinetic energy contour aroundstreamlined head.

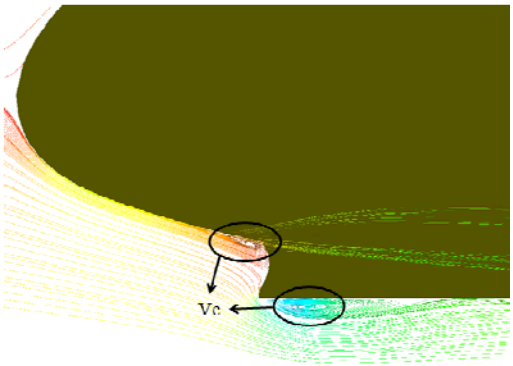

Fig. 8 Streamlines around cowcatcher.

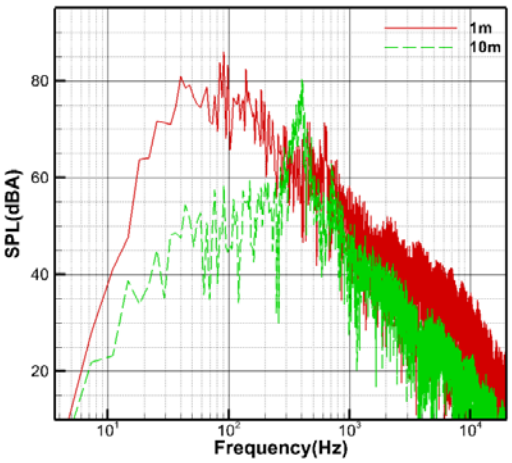

Fig. 9 Frequency spectra of probes in upstream region.

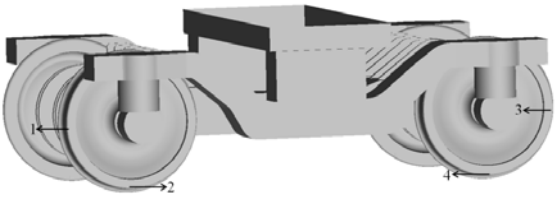

Fig. 10 Probe configuration around bogie zone.

downstream, its velocity becomes slower and the pressure along the surface of the downstream bogies turns to be uniform. Consequently, only bogie No. 1 and No. 2 are analyzed in the present paper. In the zone of each bogie, probes are placed around the wheels, and the middle and bottom of the wheels are all interested locations. At the same time, the upstream and downstream of the cover of the bogie are also selected for noise analysis. The probe configuration around the bogie is shown in Fig. 10.

Taking a close look at the bogie, it will be found that the bogie is mainly composed of two axles and four wheels. When the flow passes by the bogie, it will swirl around the axles and increase the turbulence intensity, making the bogie a remarkable noise source. Fig. 11 shows the frequency spectra for the probes around the two bogies.

As seen in Fig. 11a, the four probes on bogie No. 1 are all in a high level of aerodynamic noise, among which probe-3 locating in the middle of the downstream wheel is the highest, with a value of 128dBA. Comparative study reveals that the lowest noise appears at the bottom of the upstream wheel, but it still has a level as high as 110dBA. The aerodynamic noise in the downstream area of bogie No.1 is slightly higher than that in the upstream area, indicating that the downstream area of bogie No. 1 experiences worse noise pollution.

As Fig. 11b shows, noise level of the four different locations in the zone of bogie No. 2 seems to be similar, varying from 114dBA to 120dBA. Although they are all still at a high level, better noise circumstance could be observed than that in the zone of bogie No. 1. Due to the heavily disturbance by the components on the bogies, no distinct frequency mode could be observed. The dominant frequency ranges from 100Hz to 200Hz for bogie No. 2. The upstream area of bogie No. 2 seems to suffer more in noise circumstance than the downstream area of bogie No. 2. For example, the noise level at the bottom of the upstream wheel is a little higher than that of the downstream wheel.

4.1.3 Streamlined head of trailing car

Considering that the model is symmetrical about the origin of the coordinates, the probe configuration on the streamline of the trailing car is completely consistent with the configuration of the leading car. For simplicity, the noise analysis on the trailing car mainly focuses on the nose of the streamline and the connection part between the streamline and the cowcatcher. Comparative study between the leading car and the trailing car is performed.

The flow in the wake zone is totally different from the upstream flow. A uniform flow passes by the streamline of the leading car, while high turbulent flow goes through the streamline of the trailing car. Complicated phenomena such as flow separation and reattachment occur on the surface of the streamline of the trailing car, which will bring greater noise pollution. Fig. 12 shows the streamlines in the wake zone.

As Fig. 12 shows, two big vortices could be found stretching backward with opposite swirling directions. The streamlines in the wake zone seem more irregular and the flow here has a relatively large turbulence intensity, which will result in high aerodynamic noise.

Fig. 13 shows the frequency spectrums of the probes on the streamline of the trailing car. As shown in Fig. 13a, the two probes on the nose of the streamline of the trailing car have higher sound pressure levels compared to the corresponding probes on the leading car. The

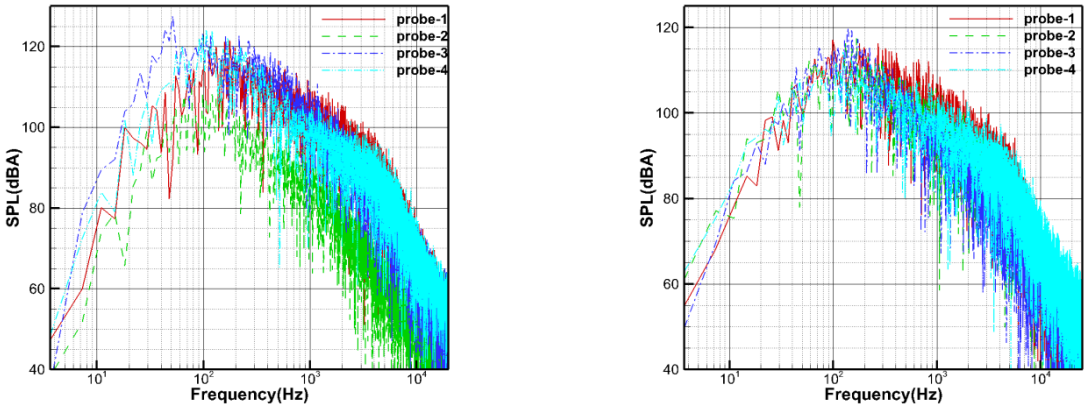

(a) frequency spectra of probes around bogie No.1

(b) frequency spectra of probes around bogie No.2

Fig. 11 Frequency spectra of probes around bogie No.1 and No.2

noise level of probe-1 is around 100dBA and the corresponding dominant frequency ranges from 100Hz to 200Hz, while probe-2 has a value of 125dBA and a dominant frequency around 100Hz. An obvious difference with the leading car could be observed that the frequency spectra of the probes on the trailing car have no distinct high frequency mode. This may be attributed to that the nose tip of the trailing car is the location where eddies detach from and the lateral separation lines reattach. Complicated flow phenomena will increase the turbulent disturbance and consequently increase the overall sound pressure level.

As Fig. 13b shows, a lower noise level of 106dBA could be found beneath the cowcatcher compared to the corresponding location on the leading car. This may be attributed to that the flow mechanisms of the two locations on the train are totally different. Fluctuations with high intensity will be found beneath the cowcatcher of the leading car due to the high speed flow developed along the surface. However this high speed flow disappears in the corresponding location of the trailing car, and mechanisms such as flow separation and reattachment come into effect. The intensity variation of the two mechanisms will result in the difference of noise levels.

As discussed above, two additional probes are placed in the wake flow with a distance of 1m and 10m backward from the nose of the trailing car. The frequency spectra of the two probes are shown in Fig. 14. The two locations still suffer from high aerodynamic noise, with a value of 105dBA and 93dBA respectively. Similar to the results of the upstream analysis, the noise level gets lower as the probe gets further away from the train. Due to the disturbance from the trail vortices, the turbulence intensity is in a relatively high level for a certain distance. As a result, they are both greater than those of the corresponding locations in the upstream flow, which are 85dBA and 80dBA, respectively.

4.2 Noise suppression

There are plenty of noise sources on the surface of a high speed train, such as the streamlined head, bogies, cab windows, cowcatchers and pantographs. Unreasonable design usually leads to a great disturbance of the flow around the train and results in high aerodynamic noise. In the present paper, only two noise sources (cab windows and cowcatchers) are chosen to be studied and several designs are exhibited. Noise analysis is performed based on these designs and in the end a new design of high speed train with low noise is proposed.

4.2.1 Cab window

As mentioned above, there are several factors that affect the noise characteristics of the high speed train, among which a key factor is the connection style between the cab window and the streamline.

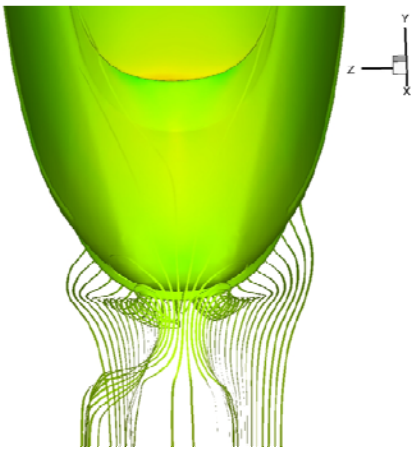

Fig. 12 Streamlines in wake zone.

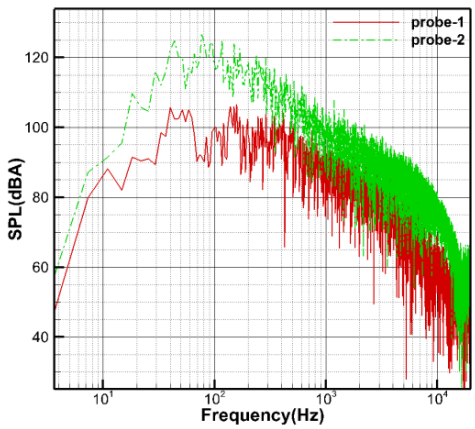

(a) frequency spectra around nose

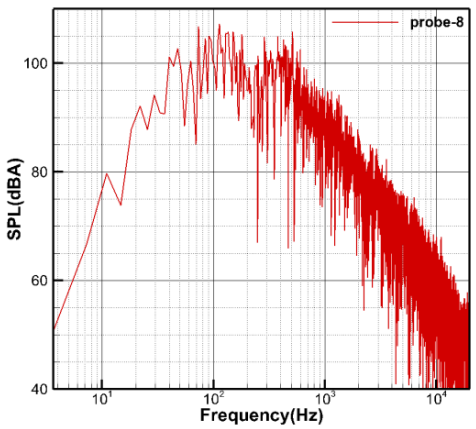

(b) frequency spectra around cowcatcher

Fig. 13 Frequency spectra around streamline of trailing car.

Unreasonable design will result in high noise. In this section several designs are proposed, as Fig. 15 shows.

As seen above, Fig. 15a shows the cab window used in above analysis of noise characteristics in near field, which is concave to the streamline. Fig. 15b utilizes a total different way of connection. The cab window is convex over the streamlined surface. Fig. 15c has improvements. In particular, a small cavity has been added at the leading edge of the cab window to ensure the smooth connection. However, a sharp edge exists at the trailing of the cab window. Fig. 15d guarantees the smooth connection between the cab window and the streamline at the outer surface. However, a large gap and a sharp edge exist at the leading edge of the cab window. In present paper, noise analysis of the four designs has been performed and the highest noise level generated by these designs is shown in Fig. 16 for comparison.

The highest noise level generated by these four designs occurs at different locations. Design-1 generates the biggest noise at the bottom of the cavity which is just in front of the cab window. For design-2 and design-4, the worst situation occurs on the top of the convex leading edge of the cab window. For design-3, the highest noise level occurs just in front of the connection part between the cab window and the streamline. As seen in Fig. 15, the four designs could be sequenced as design-4 > design-2 > design-1 > design-3 in a manner from the highest level to the lowest. The noise level of design-4 is around 126dBA. The energy of design-4 is mainly in the band higher than 1000Hz. Design-3 is the best design among these four designs. Due to the slightly smooth connection between the cab window and the streamline in the leading edge, the biggest noise level is only about 105dBA. However, because of the existence of the shape edge in the trailing edge of the cab window, the noise level at the trailing edge is a little higher, which limits its application. Further improvement on the trailing edge of the cab window should be performed. If only a smooth connection between the trailing edge of the cab window and the streamlines is ensured, design-3 would be the best low noise design.

4.2.2 Cowcatcher

The upstream flow could be easily disturbed by the cowcatcher and generates high turbulence intensity, resulting in high noise level. In certain conditions the noise due to the disturbance of the

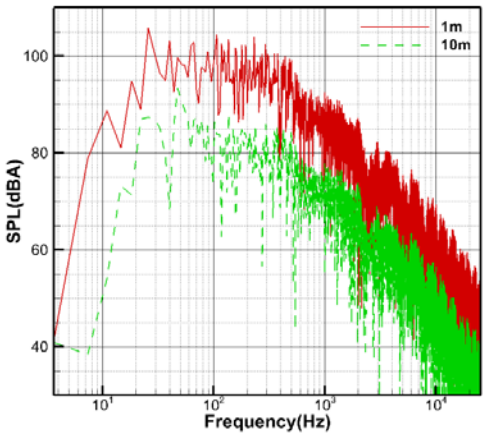

Fig. 14 Frequency spectrums of the probes in the wake zone.

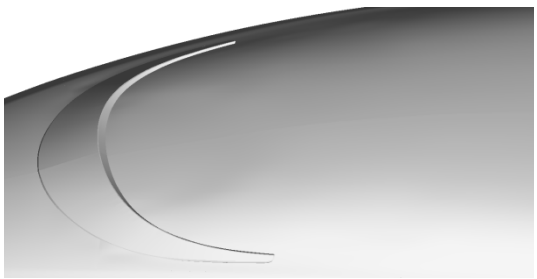

(a) design-1

(b) design-2

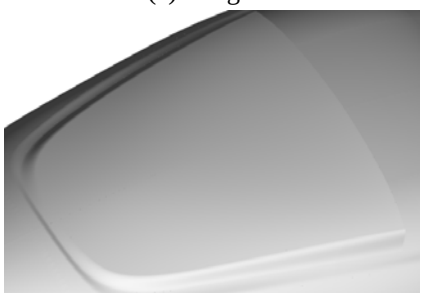

(c) design-3

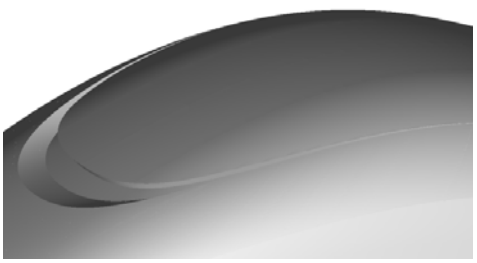

(d) design-4

Fig. 15 Different designs of cab windows.

cowcatcher may exceed the noise generated by the nose of the streamline. As a result, it will be of great importance to design the shape of the cowcatcher correctly. Several designs of the cowcatcher are proposed in Fig. 17 and the noise characteristics of these cowcatchers have also been investigated.

As seen in Fig. 17, design-1 utilizes the sheet structure as the cowcatcher, heading its leading edge directly towards the upstream flow. Design-2 is almost the same with design-1 except that an additional plank is adopted as the bottom of the cowcatcher. Design-3 and design-4 are not sheet structures. However, compared to design-2 they gradually reduce the facing angle between the upstream flow and the leading edge of the cowcatcher. Design-4 adopts a streamlined structure at the leading edge so as to minimize the disturbance to the flow. The frequency spectra of the probes where the highest noise level occurs for different designs are shown in Fig 18.

As shown in Fig. 18, design-1 with the sheet structure produces the highest noise, which occurs just in front of the leading edge with a value of around 129dBA. For design-2, due to the large facing angle between the upstream flow and the leading edge, the flow experiences high turbulence intensity there. As a result, the noise level is still at a high level, which is about 120dBA. After gradually reducing the facing angle, as design-3 and design-4 do, the noise level has been effectively suppressed. For design-3 the highest noise level is about 116dBA. For design-4 a streamlined structure has been achieved and its highest noise level is 109dBA, which is the best design of all. Results reveal that low noise design of the cowcatcher should avoid using the sheet structure and keep a streamlined structure.

4.3 Optimal design of high speed train with low noise

Based on the above analysis, in order to suppress the noise level of the high speed train, the cab window should use design-3 in section 4.2.1. The trailing edge of the cab window should be kept smooth with the streamline. For the design of cowcatchers, design-4 in section 4.2.2 should be utilized so as to minimize the disturbance to the flow. Based on the prototype, the cab window and the cowcatcher have been revised under the above analysis. The new design of the high speed train is shown in Fig. 19.

As Fig. 19 shows, the new streamlined head has achieved further improvement compared to the prototype head. In order to investigate the noise

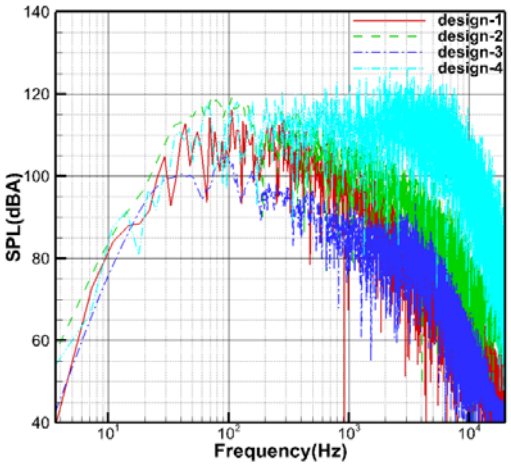

Fig. 16 Frequency spectra of probes with highest noise level for different designs.

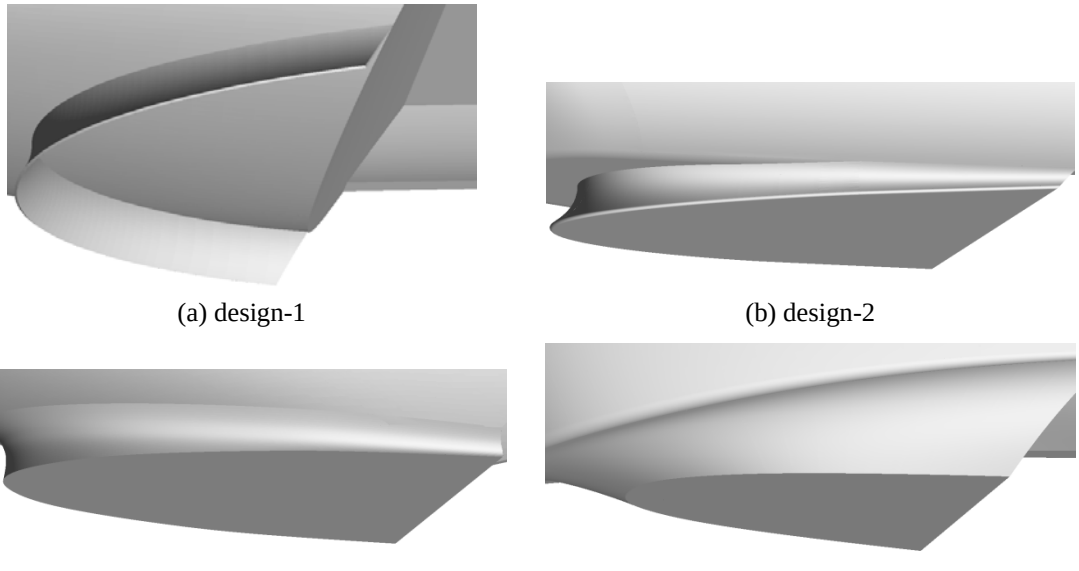

(a) design-1 (b) design-2

(c) design-3 (d) design-4

Fig. 17 Different designs of cowcatchers.

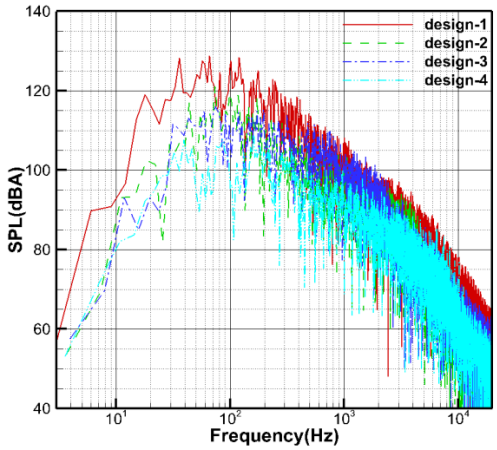

Fig. 18 Frequency spectrums of the probes with the highest noise level for different designs.

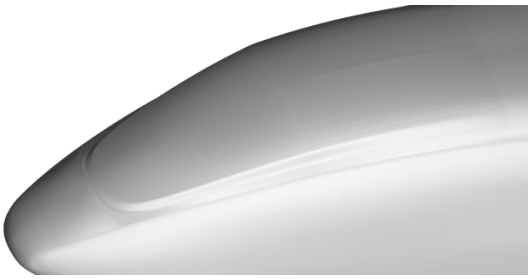

(a) cab window

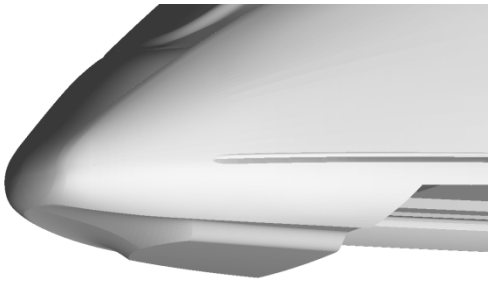

(b) cowcatcher

Fig. 19 Optimal design of high speed train.

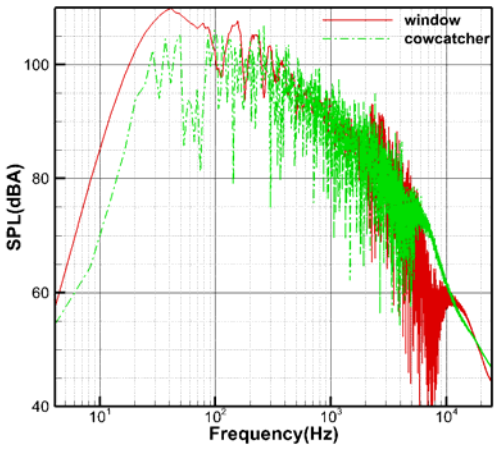

Fig. 20 Frequency spectra with high noise level in specific locations.

characteristics of the new high speed train, numerical simulation of the new design has been performed. In order to minimize the numerical error, the mesh configuration and computational conditions are both kept the same as the prototype. The noise characteristics around the cab window and the cowcatcher are the focus of this section. The frequency spectra with the highest noise level at these two locations are shown in Fig. 20.

As Fig. 20 shows, the worst situation around the cab window occurs in the cavity in front of the cab window, where its highest noise level is 110dBA. The highest noise level around the cowcatcher appears at the bottom of the leading edge of the cowcatcher with a value of 107dBA. Compared to the prototype, whose highest noise levels around the cab window and the cowcatcher are 117dBA and 121dBA, respectively, the noise levels of the new designed train have been reduced by 7dBA and 14dBA, respectively. Computational results reveal that the noise level of the new designed train has been greatly suppressed by revising the shape of the cab window and the cowcatcher. The new designed high speed train could be assumed to be a low noise train.

5. CONCLUSIONS

The noise characteristics of the CRH3 high speed train have been numerically simulated, and the streamlined head of the leading car, the cab window, the cowcatcher, the bogies and the streamlined head of the trailing car are the main concern. Several designs of cab windows and cowcatchers have been proposed. Through the comparative study of these designs, low noise designs of these components have been selected. In the end, a new high speed train with low noise is suggested. Several conclusions have been obtained.

1. Main noise sources include the streamlined shape, cowcatchers and the bogies. Highest noise of the streamlined head of the leading car occurs at the connection part between the streamline and the cowcatcher. Aerodynamic noise in the downstream area of bogie No. 1 is slightly higher than that in the upstream area. The variation of the noise level in the zone of bogie No.2 seems to be small, compared to that in the zone of bogie No.1. Due to the higher turbulence intensity around the nose of the trailing car, the noise level at the nose of the trailing car is a little higher than that at the nose of the leading car.

2. The turbulence intensity is a key factor that influences the aerodynamic noise of the high speed train. The higher the turbulence intensity gets, the stronger the aerodynamic noise is. Some factors could directly affect the turbulence intensity, which include the flow velocity, flow separation and flow reattachment.
3. In order to design a high speed train with low noise, a smooth connection between the cab window and the streamline should be ensured. In the designs proposed in present paper, design-3 is the best low noise design. However, the trailing edge of the cab window in design-3 should be further improved so as to attain smooth connection.
4. Incorrect design of cowcatchers will result in high aerodynamic noise. A low noise design of the cowcatcher should avoid the use of sheet structures and decrease the facing angle between the cowcatcher and the upstream flow so as to minimize the disturbance to the flow.
5. Based on the prototype of the CRH3 high speed train, a new design of high speed trains with low noise has been proposed. The new train has its cab windows and cowcatchers further improved. Compared to the prototype, the new design has the noise levels reduced by 7dBA and 14dBA at the cab window and the cowcatcher, respectively.

ACKNOWLEDGEMENT

This work is supported by the National Science and Technology Pillar Program during the Eleventh Five-Year Plan Period (No.2009BAG12A03) and the National Key Basic Research and Development Program (973 program) (No.2011CB711101).

REFERENCES

1. Batten P, Ribaldone E, Casella M, Chakravarthy S (2004). Towards a generalized non-linear acoustics solver. *10th AIAA/CEAS Aeroacoustics Conferences*.
2. Batten P, Goldberg U, Chakravarthy S (2002). Reconstructed sub-grid methods for acoustics predictions at all reynolds numbers. *8th AIAA/CEAS Aeroacoustics Conference and Exhibit*. Breckenridge, Colorado.
3. Casper J, Farassat F (2002). A new time domain formulation for broadband noise predictions. *International Journal of Aeroacoustics* 1(3):207-240.
4. Casper J, Farassat F (2002). Broadband noise predictions based on a new aeroacoustic formulation. *40th AIAA Aerospace Sciences Meeting and Exhibit*.
5. Curle N (1955). The influence of solid boundaries upon aerodynamic sound. *Philosophical Transactions of the Royal Society of London, Series A, Mathematical and Physical Sciences* 231(1187):505-525.
6. Ffowcs-Williams JE, Hawkings DL (1969). Sound generation by turbulence and surfaces in arbitrary motion. *Philosophical Transactions of the Royal Society of London, Series A, Mathematical and Physical Sciences* 264(1151):321-342.
7. Lighthill M J (1952). On sound generated aerodynamically. I. General theory. *Philosophical Transactions of the Royal Society of London, Series A, Mathematical and Physical Sciences* 211(1107):564-587.
8. Lighthill M J (1954). On sound generated aerodynamically. II. Turbulence as a source of sound. *Philosophical Transactions of the Royal Society of London, Series A, Mathematical and Physical Sciences* 222(1148):1-32.
9. Mellet C, Letourneaux F, Poisson F, Tallotte C (2006). High speed train noise emission: Latest investigation of the aerodynamic/ rolling noise contribution. *Journal of Sound and Vibration* 293:535-546.
10. Merci B, Vierendeels J, Langhe C D, et al (2001). Development and application of a new cubic low-Reynolds eddy-viscosity turbulence model. *31st AIAA Fluid Dynamics Conference & Exhibit*.
11. Moritoh Y, Zenda Y and Nagakura K (1996). Noise control of high speed Shinkansen. *Journal of Sound and Vibration* 193(1):319-334.
12. Nagakura K (2006). Localization of aerodynamic noise sources of Shinkansen trains. *Journal of Sound and Vibration* 293:547-556.
13. Noger C, Patrat JC, Peube J, Peube JL (2000). Aeroacoustical study of the TGV pantograph recess. *Journal of Sound and Vibration* 231(3):563-575.
14. Sun ZX, Song JJ, An YR (2012). Numerical simulation of aerodynamic noise generated by high speed trains. *Engineering Applications of Computational Fluid Mechanics* 6(2):173-185.

15. Talotte C (2000). Aerodynamic Noise: A critical survey. *Journal of Sound and Vibration* 231(3):549-562.
16. Talotte C, Gautier PE, Thompson DJ, et al (2003). Identification, modelling and reduction potential of railway noise sources: A critical survey. *Journal of Sound and Vibration* 267:447-468.